Pf1 bacteriophage hydration by magic angle spinning solid-state NMR

Cite as: J. Chem. Phys. **141**, 22D533 (2014); https://doi.org/10.1063/1.4903230
Submitted: 05 September 2014 . Accepted: 12 November 2014 . Published Online: 09 December 2014

Ivan V. Sergeyev, Salima Bahri, Loren A. Day, and Ann E. McDermott

Pf1 bacteriophage hydration by magic angle spinning solid-state NMR

Ivan V. Sergeyev,[1] Salima Bahri,[1] Loren A. Day,[2] and Ann E. McDermott[1,a)]
[1]*Department of Chemistry, Columbia University, 3000 Broadway, New York, New York 10027, USA*
[2]*Public Health Research Institute, Rutgers University, 225 Warren St., Newark, New Jersey 07103, USA*

(Received 5 September 2014; accepted 12 November 2014; published online 9 December 2014)

High resolution two- and three-dimensional heteronuclear correlation spectroscopy (^{1}H–^{13}C, ^{1}H–^{15}N, and ^{1}H–^{13}C–^{13}C HETCOR) has provided a detailed characterization of the internal and external hydration water of the Pf1 virion. This long and slender virion (2000 nm × 7 nm) contains highly stretched DNA within a capsid of small protein subunits, each only 46 amino acid residues. HETCOR cross-peaks have been unambiguously assigned to 25 amino acids, including most external residues 1–21 as well as residues 39–40 and 43–46 deep inside the virion. In addition, the deoxyribose rings of the DNA near the virion axis are in contact with water. The sets of cross-peaks to the DNA and to all 25 amino acid residues were from the same hydration water ^{1}H resonance; some of the assigned residues do not have exchangeable side-chain protons. A mapping of the contacts onto structural models indicates the presence of water "tunnels" through a highly hydrophobic region of the capsid. The present results significantly extend and modify results from a lower resolution study, and yield a comprehensive hydration surface map of Pf1. In addition, the internal water could be distinguished from external hydration water by means of paramagnetic relaxation enhancement. The internal water population may serve as a conveniently localized magnetization reservoir for structural studies.
 [http://dx.doi.org/10.1063/1.4903230]

INTRODUCTION

Understanding the hydration of proteins and nucleic acids is an important part of understanding their structures and functions. The inherent differences between hydration water and liquid water are widely recognized. In liquid or bulk water, the first shell around a central water molecule has between four and five water molecules, as shown by oxygen-oxygen pair correlation functions at short distances. By contrast, water on the surface of a macromolecule will have fewer water neighbors, different dynamics, and different H-bonding options, all dependent on the context.[1,2] These effects lead to notable depressions in freezing points, or even an inability to freeze.[3–5] NMR studies of hydration have the added complexity that the chemical shift of a given hydration water proton is averaged with the chemical shift of bulk water protons. This averaging arises because the binding and release of the surface water molecules is normally fast (ns–μs) compared to NMR measurement timescales (ms).[1,6–10] Nevertheless, surface water has been effectively studied by NMR. Relaxation measurements have been made of protein hydration sites that exhibit hindered water rotation.[1,6,11] Correlation of water to protein NMR peaks via the nuclear Overhauser effect (NOE) has also been used in both solution and solid state NMR (SSNMR).[1,12] Partially dehydrated samples having increased fractions of hydration water, and frozen samples having only the hydration water, give rise to liquid-like NMR spectra for the hydration shell.[9,13,14] Another approach has been to confine macromolecules in smaller pools of water, including inverted micelles,[15,16] organic solvents,[17–19] ice encapsulation,[14,20,21] and model systems such as capillaries.[22,23] The primary NMR relaxation mechanism of confined and/or bound water is clearly different from that of bulk water;[24–26] the correlation times of water molecules bound in the interior of a protein tend to be on the microsecond timescale at room temperature.[6,7,27] The dynamics of surface hydration waters are highly heterogeneous and differ in temperature dependence. Often, a few secluded sites are dominant in the overall NMR data. On average, at room temperature, the hydration water can be considered hindered with respect to rotation and translation. In contrast, at lower temperatures, the surface water appears to be relatively mobile as compared with ice (or even supercooled water).[5,14]

Pf1 bacteriophage, discovered a half century ago,[28] has become one of the paradigms of filamentous phage structure. Its long thin virion (2100 nm × 7 nm) has a loop of single-stranded circular DNA of 7349 nucleotides within a shell of ∼7300 major coat protein subunits, each only 46 amino acids. At the ends are reverse turns of the circular ssDNA and a few copies of proteins that are important to virus function but that are not directly related to the present study. The subject here is the hydration of the major coat protein and the DNA, which together constitute 99% of the 36 MDa virion dry mass (93% major coat protein, 6% DNA). Extensive results from previous studies have established many aspects of Pf1 structure.[29–33] The protein subunits are largely α-helical and their close packing presents a negatively charged grooved outer surface at 30–35 Å radius, a hydrophobic region centered at 20 Å radius, and a positively charged inner protein surface at about 10 Å radius from the central axis. The Pf1 DNA structure is proposed to have the antiparallel sugar-phosphate backbones in contact at the axis, with the phosphorous atoms at 2.5 Å radius and the bases directed

a)Author to whom correspondence should be addressed. Electronic mail: aem5@columbia.edu. Fax: 212-932-1289.

outward. This model was based on a matching of DNA and capsid helical symmetries to account for the 1:1 chemical ratio of nucleotides to coat protein subunits as well as spectroscopic data,[29,34] analyses of electrostatic repulsion,[35] and electron density.[36] It is supported and augmented by Raman vibrational spectroscopy of oriented samples,[33] and by DNA chemical shift data obtained via dynamic nuclear polarization (DNP) enhanced solid state NMR.[37] Other work has established that Pf1 is very stable across broad ranges of temperature, pH, and ionic strength,[28,38,39] yet undergoes a cooperative phase transition at 10 °C between high- ($Pf1^H$) and low-temperature ($Pf1^L$) forms having slightly different overall helical symmetries.[40–42] This structural plasticity must involve hydration water. Further, fiber diffraction and NMR data are profoundly affected by hydration levels, motivating the desire to better understand the structure and role of hydration water in Pf1.[9,37,43]

The hydration level of Pf1 is high due to its extensive α-helical surfaces and its extended DNA conformation. For example, in the absence of the protein shell, it was estimated that 14 waters can contact each nucleotide.[44] Comparison values for dsDNA range from 4 to 10 waters per nucleotide, according to classic studies by gravimetric methods, by self-diffusion of water, and by X-ray crystallography.[45–47] With respect to the protein, which contributes 93% of the virion's dry mass, one might expect approximately one hydration water molecule per amino acid residue, as observed for average proteins.[45,48–50] Estimates presented herein for the Pf1 capsid indicate significantly higher levels overall, and ratios of external to internal hydration water of about 3 (Table S1 and Figure S1 in the supplementary material[100]). Thus, both internal and external hydration waters were expected to be readily observable, though not necessarily distinguishable, by SSNMR. The possibility of an internal hydration pool in narrow spaces between the protein coat and the DNA might provide an experimentally convenient system to investigate biologically relevant encapsulated/confined water. However, it is important to consider the degree and timescale of confinement. The dynamics of the coat protein might be expected to allow for water exchange from the outside to the inside, and clear evidence for diffusion of ions from the outside to the inside of the virus has been reported.[51,52] At the outset of our experiments, the timescale of such exchange was an open question. In the fast limit, any NMR signal from the internal water would not be directly observable; in the slow limit, we would expect the properties of the internal hydration water NMR line to be different from those of bulk water. Differences in environment as well as the density and numbers of hydrogen bonds would be expected to broaden and possibly shift the line substantially.[53]

Magic-angle spinning (MAS)-SSNMR has emerged as a principal technique for the study of structure and dynamics in complex biomolecular systems (reviewed in Refs. 54 and 55), and the roles of water in these systems have been increasingly studied by this method. Pioneering solution NMR work on hydration dynamics and localization via NOE measurements[1,56,57] gave rise to a handful of SSNMR studies of hydration and water dynamics in biological polymers,[58–62] which in turn have led to a growing body of recent SSNMR water studies in systems as diverse as bone, silica, and amyloid fibrils.[9,13,63–66] In such studies, SSNMR is often able to give site-specific information regarding solvent accessibility, chemical exchange, and dynamics.[14,63,67–72] SSNMR methods for the study of water have focused around two basic approaches: T2′ or multiple quantum filtering and dephasing of $^{13}C/^{15}N$-bound protons via rotational echo double resonance (REDOR) or similar experiments.[63,67,68,72,73] These approaches are conceptually similar in that, upon creating ^1H polarization and allowing it to diffuse, filtering or dephasing elements serve to remove unwanted magnetization. In the case of filtering, signals with fast relaxation properties are edited out (water proton signals generally relax slowly); in the case of dephasing, magnetization from protons directly bonded to ^{13}C or ^{15}N is dephased by the recoupling of their dipolar interactions. The net effect in both cases is to isolate magnetization arising from water, which can be detected directly in ^1H-detected experiments, or transferred to nearby ^{13}C or ^{15}N nuclei, which provide superior site-resolution for detection. Additional resolution can also be gained by adding dimensions, for instance, by adding ^{13}C–^{13}C homonuclear recoupling elements to provide additional information on ^{13}C connectivity.

An initial SSNMR study of Pf1 water accessibility was carried out by Purusottam and co-workers,[74] who used ^1H–^{15}N heteronuclear correlation (HETCOR) spectroscopy to identify hydrated residues. The chemical shift dispersion of ^{15}N, however, is inherently lower than that of ^{13}C, largely precluding reliable assignments in congested regions of the spectrum based on ^{15}N chemical shift alone. In the present study, we applied two- and three-dimensional ^{13}C-based SSNMR techniques, with the addition of efficient ^1H homonuclear decoupling, to rigorously assign water populations, to map water-exposed residues in the major coat protein, and to probe whether the DNA is water-exposed in $Pf1^L$. We also introduce a strategy based on paramagnetic relaxation enhancement (PRE) to differentiate internal hydration water from external hydration water.

MATERIALS AND METHODS

Uniformly isotopically enriched U–^{13}C, ^{15}N–Pf1 was prepared as previously described.[75] Several different samples were used for this work, however, the preparation was the same in all cases. This included recovery of purified Pf1 bands from cesium chloride density gradient centrifugation runs. To fill the MAS rotors for NMR experiments, 12 mg of purified U–^{13}C, ^{15}N–Pf1 were precipitated from 200 mM TRIS buffer (pH 8.4) by the addition of 8% w/v PEG-8000 and 5 mM $MgCl_2$. Precipitation was allowed to complete over several hours at 4 °C, and the precipitate was collected by centrifugation at 6200 g for 20 min. Precipitate was kept in an Eppendorf tube and placed into a custom-built constant flow hydration chamber, where the humidity of air passing over the sample was kept constant at 90% relative humidity (RH) at room temperature. A given sample was allowed to equilibrate with the air over 7–8 h, during which time the equilibration was monitored by sample mass loss (data points taken every half hour). When no mass change had been observed for 3 subsequent data points, the sample was considered to have

equilibrated to 90% RH. The sample was then transferred to a 3.2 mm Bruker solid-state NMR rotor by slow centrifugation (4 m at 2000 g). For the Pf1 sample used in paramagnetic relaxation enhancement experiments, 3 μl of 200 mM TmDOTP stock solution was added to a sample volume of approximately 45 μl; the volume was reduced to 30 μl after hydration control, for an effective relaxant concentration of 20 mM.

Spectra were acquired on Bruker AVANCE III 400 MHz and 600 MHz spectrometers, as well as Bruker AVANCE II 750 MHz and 900 MHz spectrometers, using 3.2 mm triple-channel MAS probes in all cases. The MAS rates used varied from 8.0 to 18.5 kHz, and were selected to optimize spinning sideband positions. Spectra were acquired at a variety of temperatures from −20 °C to 25 °C. 90–100 kHz SPINAL-64[76] proton decoupling was used during ^{13}C acquisition in all cases. The pulse sequences used for acquisition are shown in Figure 1. Many of these are elaborations on the basic HETCOR experiment, which, in the solid state, simply uses a cross polarization (CP) element to transfer magnetization from ^{1}H

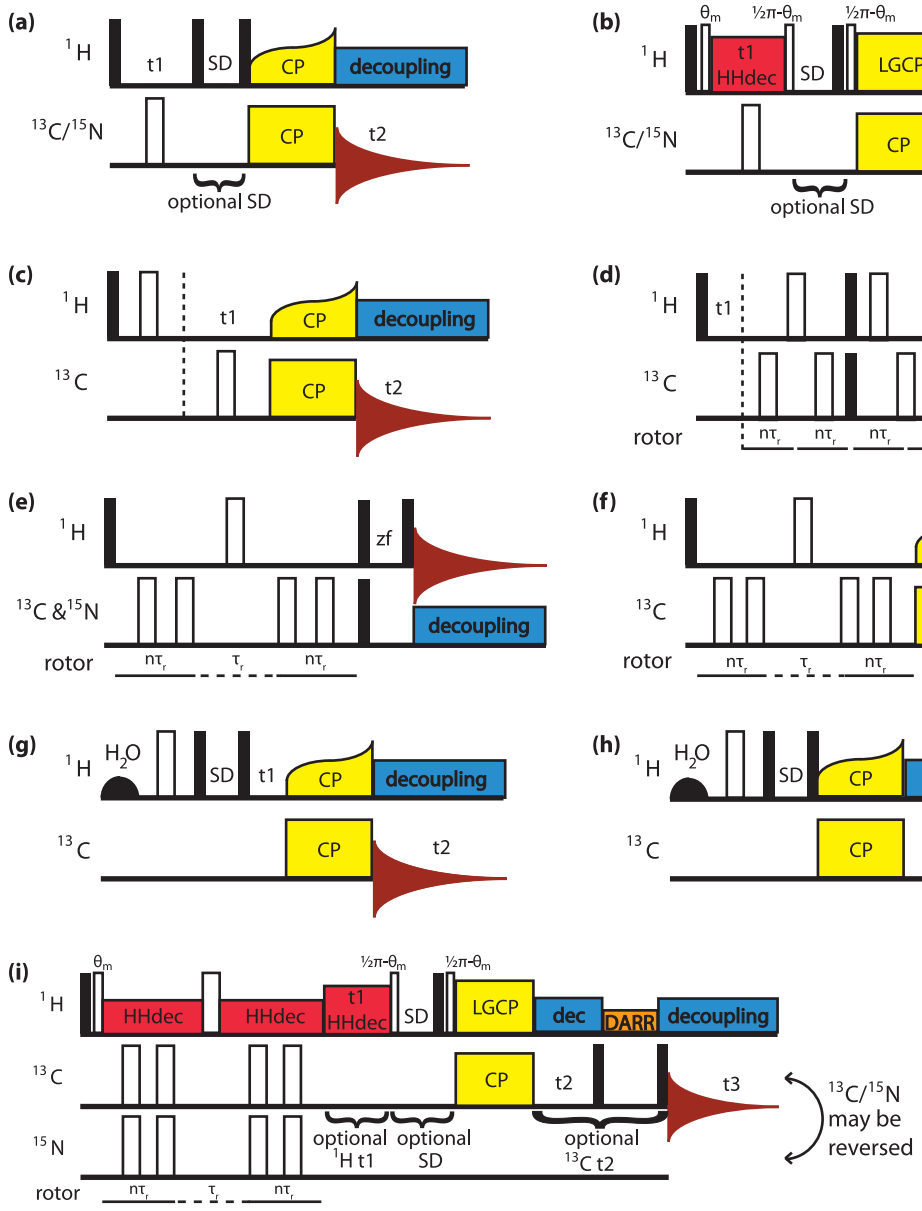

FIG. 1. Schematic representation of pulse sequences used in this work. Filled black bars represent $\pi/2$ pulses, while empty bars represent π pulses unless otherwise denoted above; all other elements are labeled accordingly. "SD" indicates a ^{1}H spin diffusion (or ^{1}H mixing) element, and "zf" a z-filter (z-filters can also be gradient-enhanced, not shown). H_2O denotes a water-selective shaped pulse (EBURP shapes were used in this work). HHdec denotes ^{1}H homonuclear decoupling; in this work, the eDUMBO-1_{22} phase program[77] with 0.5 μs phase switch time was found to be most efficient and is used for all homonuclear decoupling. All pulse programs were coded for and used with Bruker TopSpin 2.1-3.2. (a) ^{1}H–^{13}C/^{15}N heteronuclear correlation (HETCOR) with optional SD; (b) ^{1}H–^{13}C/^{15}N heteronuclear correlation (HETCOR) with homonuclear decoupling, LGCP, and optional SD; (c) ^{1}H–^{13}C heteronuclear correlation with T2′-filter (T2′-filtered HETCOR); (d) ^{1}H–^{13}C transferred echo double resonance (TEDOR); (e) ^{1}H REDOR-^{13}C/^{15}N-dephased 1D; (f) ^{1}H–^{13}C REDOR-dephased HETCOR; (g) H_2O-selective T2′-filtered ^{1}H–^{13}C HETCOR; (h) H_2O-selective T2′-filtered homonuclear ^{13}C–^{13}C dipolar assisted rotational resonance (DARR); (i) ^{1}H–^{13}C/^{15}N medium-to-long distance (MELODI) heteronuclear correlation experiment (MELODI-HETCOR),[78] with homonuclear decoupling, LGCP, and optional SD period. When the ^{1}H t1 period is employed in the absence of t2/DARR, this is the MELODI-HETCOR experiment; when t2 and DARR are enabled, and the ^{1}H t1 period disabled, this is the MELODI-DARR experiment; when all evolution periods are employed, this schematic represents the MELODI-^{1}H–^{13}C–^{13}C 3D experiment.

to a second nucleus ($^{13}C/^{15}N$ in this work). The transferred echo double resonance (TEDOR) technique was also used for magnetization transfer; though this transfer is through-space and not through-bond, it will nonetheless be most efficient between nuclei that maintain a fixed orientation and distance on the NMR timescale – in other words, for directly bonded nuclei.

The Pf1 samples used were fully protonated, in contrast to the extensively deuterated samples used to increase resolution in the proton dimension in some previous studies.[63,67] For some of the HETCOR experiments in this work, no homonuclear decoupling was used during t1, in effect filtering for protons with long T2, such as those of water. Other experiments included eDUMBO-1_{22} homonuclear decoupling[77] for improved ^{1}H resolution. Finally, moderate MAS frequencies (12–18 kHz) were used, comparable to previous studies of water by SSNMR.[63,67–69] At these MAS rates, the observed ^{1}H resolution is considerably better than expected. Fully protonated samples are expected to have broad linewidths and poor resolution at baseline in the absence of fast spinning and/or deuteration. Key proton peaks in our Pf1 data have full widths at half-height (FWHH) as low as 120 Hz/0.16 ppm.

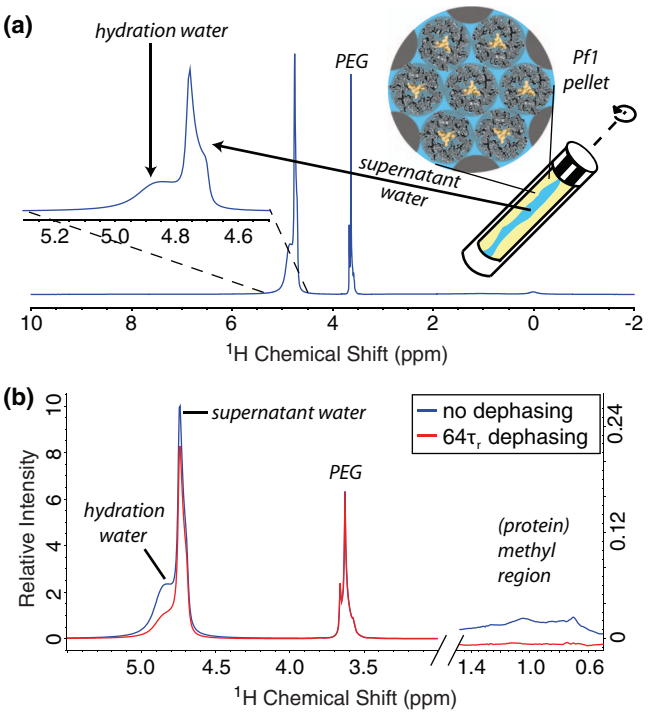

FIG. 2. (a) ^{1}H spectrum of U–^{13}C, ^{15}N–Pf1 at 0 °C and 90% relative humidity, with inset of the downfield region around 4.8 ppm. Peaks at 3.6 ppm and 1.1 ppm are assigned as PEG-8000 and coat protein methyl groups, respectively. Peaks at 4.8 and 5.0 ppm are assigned to supernatant and hydration water, respectively. The relative positions of these different water pools in a SSNMR rotor are depicted at right. (b) One-dimensional REDOR-dephasing spectra (pulse sequence shown in Figure 1(e)), with 64 rotor periods of dephasing show rapid dephasing of the signal originating from ^{13}C-attached methyl protons and partial dephasing of the hydration water peak, while other signals remain phased. A full dephasing buildup curve is shown in Figure S2 in the supplementary material.[100]

RESULTS AND DISCUSSION

Preliminary assignment of ^{1}H spectrum and ^{1}H–^{13}C correlation spectroscopy

Figure 2(a) shows the ^{1}H spectrum, acquired at 400 MHz and with 18 kHz MAS, for U–^{13}C, ^{15}N Pf1 that was equilibrated with air at 90% relative humidity before being rapidly sealed in the rotor. Assignments for supernatant water and hydration water are shown. These assignments were made initially based on chemical shift as well as linewidth, and subsequently confirmed by other methods that mirror reports by Lesage and co-workers[72] and Böckmann and co-workers[67] in studies of the dimeric protein Crh. Supernatant water refers to non-interacting water in the center of the rotor that has been squeezed out of the virus pellet by the high centrifugal fields of MAS-SSNMR experiments. It should be noted that the virus remains structurally intact and infectious under these conditions. In this report, we use the term "hydration water" to refer to any water in the pellet that is in close contact with the Pf1 virion, regardless of its residence time or position. Hydration water can be characterized by its chemical shift, downfield from that of bulk water, and its inherently broad linewidth, which is attributable to a variety of interactions with Pf1. An upfield shoulder is present on the supernatant water peak in some spectra – this is potentially an artifact due to magnetic field inhomogeneity.[67] A PEG-8000 peak (3.6 ppm) is also observed. To confirm these putative assignments, a series of 1-dimensional ^{13}C REDOR-dephasing experiments was used, similar to those used by Chevelkov and co-workers to dephase magnetization from protons directly bonded to ^{15}N while preserving magnetization arising from water.[63] The REDOR dephasing data (Figure 2(b); dephasing curves provided in Figure S2 in the supplementary material[100]) indicate that the resonances corresponding to supernatant water and PEG-8000 are not directly bonded to ^{13}C, as these peaks do not appreciably dephase. The broader hydration water peak does dephase on the ~10 ms timescale, which is indicative of it being in contact or in chemical exchange with the Pf1 coat protein, consistent with previous assignments. The signals from the protein methyl region, which can be assigned to a variety of directly ^{13}C-bonded coat protein Hδ/Hγ protons, dephases on the 1 ms timescale. This is slower than predicted for a 1-bond ^{1}H–^{13}C dipolar coupling, but simulations on an isolated spin system do not take into account complex behavior such as the ^{1}H spin bath. Further experiments to confirm these assignments were carried out, including supernatant removal, sample freezing, and exchange spectroscopy – these data are presented in the supplementary material.[100]

^{1}H–^{13}C HETCOR experiments, as shown in Figure 3(a), provide information on all possible ^{1}H–^{13}C magnetization transfer pathways in the sample. As no discrete filtering was performed, magnetization arising from water is only a small component of the overall spectrum. The addition of T2′-filtering (Figure 3(b)), with an echo delay chosen such as to filter for long T2′ (2.0 ms), retains primarily water magnetization and greatly simplifies the spectrum, though a few narrow peaks arising from directly bonded ^{1}H–^{13}C pairs (e.g., methyl groups) remain in the 0–2 ppm range. These ^{1}H peaks are unusually sharp for a fully protonated sample, and can largely be assigned to N-terminal residues, suggesting that the

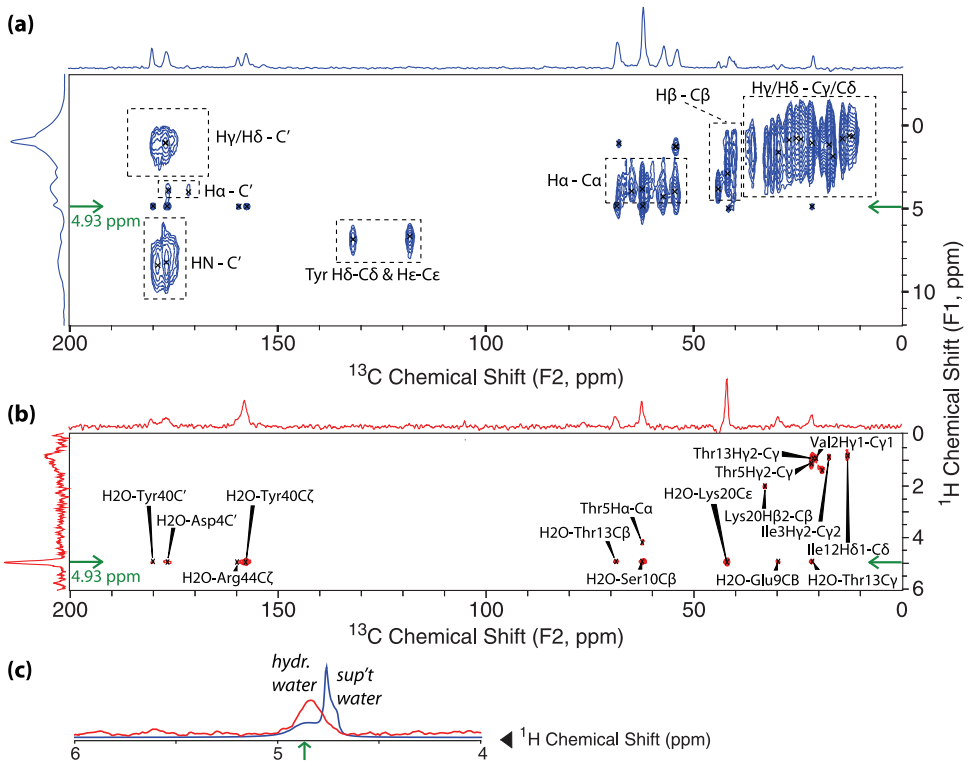

FIG. 3. (a) 2D HETCOR spectrum (pulse sequence shown in Figure 1(a): 1 ms CP contact time) of Pf1, with intrinsic resolution of 75 Hz/0.1 ppm and 187 Hz/0.8 ppm in the ^{1}H and ^{13}C dimensions, respectively. The position of the 4.93 ppm hydration water ^{1}H resonance is marked with green arrows to highlight water-protein cross-peaks. The horizontal projection is the sum of the ^{13}C slices that make up the FWHH of the water resonance in the indirect dimension; the vertical projection represents the sum of all ^{1}H slices. The supernatant water resonance has an irregular lineshape, consistent with previous observations.[67] For non-water ^{1}H resonances, dashed rectangles show generic assignment groups. (b) The T2′-filtered HETCOR spectrum (pulse sequence shown in Figure 1(c)) of Pf1 restricts cross-peaks to primarily those arising from hydration water, resulting in a much sparser spectrum. Assignments were made based on existing chemical shift tables for the Pf1 major coat protein. Unsurprisingly however, the filtered version does not reveal any new cross-peaks not present in the conventional HETCOR. (c) Overlay of ^{1}H spectrum of U–^{13}C, ^{15}N Pf1 shown in Figure 2(a) (blue) upon the ^{1}H projection from T2′-filtered HETCOR (red), showing the greatly increased prevalence of hydration water signal relative to supernatant water in T2′-filtered spectra. All spectra were taken at 0 °C.

N-terminus of the coat protein exhibits a high degree of mobility. The latter is consistent with hydrodynamic measurements on similar phages, which reveal hydrodynamic radii considerably larger than the corresponding fiber diffraction radii,[79] presumably due to N-terminal plasticity of the coat and interactions with water in wet samples. The position of the hydration water resonance is indicated with green arrows to highlight hydration water-protein cross-peaks. The majority of these water cross-peaks have ^{1}H linewidths in excess of 100 Hz (Figure 3(c)), closely matching the linewidth of hydration water in 1-dimensional spectra (∼120 Hz/0.16 ppm). It is noteworthy that the CP contact times used in Figure 3 were long (900 μs), allowing for chemical exchange from water. With more selective short CP contact times (200–350 μs) as used in the bulk of this work, water contacts are not observed unless a ^{1}H mixing (or spin diffusion) period is added. The significance of this will be discussed in subsequent sections.

Analysis of the ^{13}C cross-peaks to the hydration water resonance in Figures 3(a) and 3(b) reveals peaks at 159.9 ppm, which, in the context of Pf1, can only be assigned as Arg44-Cζ of the coat protein. Tyr40-Cζ and Tyr40-C′ cross-peaks at 158.1 and 180.0 ppm, respectively, are also observed. Arg44 and Tyr40 are both located close to the C-terminal end of the 46-residue major coat protein, with their sidechains pointing inward toward the central cavity of the virion and the DNA, indicating that magnetization originating at hydration water is able to sample the virion's central cavity. The rest of the ^{13}C signals detected in the HETCOR spectra are largely attributable to externally positioned (N-terminal) residues with exchangeable sidechain protons, including Asp4, Thr5, Glu9, Ser10, Thr13, and Lys20. These residues generally exhibit intensities comparable to those of other coat protein peaks in previously published Pf1 spectra,[75] but are greatly enhanced here. The important role of chemical exchange processes in magnetization transfer under these conditions is thus consistent with conclusions from other systems.[72]

The mechanisms of water-to-protein magnetization transfer deserve mention; these have been extensively investigated in the contexts of biomolecular NMR, magnetic relaxation dispersion, and MRI.[7,8,12,16,63,72,73,80] There are three main mechanisms by which water ^{1}H polarization can be transferred to a biomolecule: chemical exchange-mediated transfer, NOE transfer, and intermolecular dipolar contact. Of the three, dipolar transfer mechanisms are unlikely in Pf1 samples,[72] as liquid (or non-crystalline) hydration water on the surface of biomacromolecules has short residence times[10,81] and low correlation times due to fast tumbling.[8,82] Because it does not depend on chemical kinetics, NOE transfer is generally rapid, yielding observable effects on the

low-millisecond timescale.[12,83] In solution NMR, the analysis of water-protein NOEs, especially with regard to water residence times, is greatly complicated by long-range coupling to bulk water.[11,84] This effect is less evident in the solid state, as there is simply less bulk-like water, and much of this is physically separated into the center of the rotor ("supernatant water") by the high centrifugal forces of even moderate MAS rates. Transfer by chemical exchange is on par with NOE mechanisms, with exchangeable amino acid sidechains having exchange times in the low millisecond range,[80,85] and backbone amides having exchange times on the order of 5–85 ms.[86–88] Because of the extreme amide pK, amide chemical exchange must typically be catalyzed by hydronium or hydroxide species, while sidechain exchange events can be catalyzed directly by water, and are therefore considerably faster at close-to-neutral pH.[89] On the timescale of an average NMR experiment (10–20 ms), it is therefore expected that chemical exchange to exchangeable sidechains and NOE transfers will be the dominant mechanisms.[12,73] While distinguishing between and/or quantifying these two mechanisms is beyond the scope of this work, it is important to note that the presence of one or both mechanisms, as indicated by the presence of a protein-water NMR cross-peak to a particular residue, is evidence of that residue being water-accessible. Chemical exchange-based transfer implies that a water molecule was sufficiently close to the residue to participate in proton exchange, while cross-peaks due to NOE transfer indicate that the water molecule was within the NOE detection limit (<4–5 Å) of the indicated residue.[16,90] Mapping such water accessibility is the chief focus of this study. While longer-range (i.e., inter-residue) relayed magnetization transfers cannot be strictly ruled out, spin diffusion and contact times have been kept as short as possible in this work to minimize such transfers, and we see no evidence of long-range non-specific cross-peaks from water, for instance, to the hydrophobic region of the coat protein.

In order to independently establish that key peaks such as Arg44-Cζ indeed represent water contacts, REDOR dephasing was used to dephase magnetization originating from protons directly bonded to ^{13}C and ^{15}N, leaving only magnetization originating from water. Conversely, the TEDOR technique, which transfers magnetization via a train of refocusing pulses, was used to transfer only magnetization from bonded ^{1}H–^{13}C pairs; water molecules are too mobile for any ^{1}H–^{13}C dipolar couplings to be effectively refocused. As a result, the TEDOR experiment represents a control for magnetization originating from ^{13}C-bound protons, clearly highlighting signals not attributable to water. As shown in Figure 4, one-dimensional ^{13}C-REDOR dephased HETCOR spectra (pulse sequence shown in Figure 1(f)) show intense peaks at 159.9 ppm and 158.3 ppm (Arg44-Cζ and Tyr25/40-Cζ), similar to those observed at the hydration water resonance in 2D HETCOR spectra. TEDOR spectra notably lack this peak. The presence of the Arg44-Cζ cross-peak in the water (4.84 ppm) slice of 2D HETCOR spectra, along with the absence of any Arg44 Hε/Hη–Cζ cross-peaks in these spectra, suggests that the peak at 159.9 ppm represents a hydration water–Arg44Cζ contact (relayed transfer through Arg44-Hε/Hη is discussed later). This observation provides additional evidence for direct water-protein magnetization transfer at the C-terminus of the major coat protein and in the interior cavity of the Pf1 virion.

Water-selective and water-filtered spectroscopy

In the interests of further improving resolution and isolating strictly the water contacts, HETCOR experiments were made water-selective by the addition of an initial shaped pulse and T2′-filter as shown in Figure 1(g).[91,92] To aid in assignment, a water-selective variant of the homonuclear ^{13}C–^{13}C pulse sequence DARR was also utilized (pulse sequence shown in Figure 1(h), data in Figure 5(b)), which allowed sequential "backbone walks" between the HETCOR and DARR. While DARR permits ^{13}C–^{13}C dipolar mixing, the indirect ^{13}C dimension represents magnetization encoded before such mixing, therefore maintaining selectivity for water contacts. These experiments also make use of a short CP for selectivity, and therefore require a ^{1}H spin diffusion element to transfer water magnetization to the coat protein. The resulting HETCOR spectra show a number of clearly assignable water-protein cross-peaks; assignments of these peaks reveal a large number of N-terminal residues with exchangeable ^{1}H sites including Gly1, Asp4, Thr5, Glu9, Ser10, Thr13, Gln16, and Lys20. Like standard HETCOR experiments, they also reveal cross-peaks to sites not expected to be exposed to external water, such as Tyr40, Arg44, and the DNA. Use of a DARR ^{13}C–^{13}C spin diffusion element in the pulse sequence expands the list of observed residues to a number of residues neighboring the aforementioned exchangeable sites. Comparison of these spectra to standard Pf1 DARR spectra reveals that N-terminal (externally facing) sites are significantly enhanced in water-selective experiments, while the vast majority of resonances from the central and C-terminal (internally facing) portions of the coat protein are almost completely suppressed. This is consistent with the water accessibility of these sites predicted from existing structural models.

Water-selective experiments, in utilizing a T2′-filter to isolate the sharper water ^{1}H signal, can however suppress some fainter cross-peaks. As a result, it is useful to compare results from water-selective spectra to those from a second and complementary class of experiments for assessing water accessibility – MELODI (MEdium-to-LOng DIstance)-HETCOR.[78,93] The MELODI-HETCOR pulse sequence (Figure 1(i)) begins by dephasing initial ^{1}H magnetization using a REDOR train of π pulses on both the ^{13}C and ^{15}N channels. In so doing, it filters out all magnetization from ^{13}C–^{1}H and ^{15}N–^{1}H spin pairs, while preserving ^{1}H magnetization on water. Some methyls cannot be effectively dephased by this scheme due to their dynamics, and therefore also retain magnetization. Once magnetization has been filtered in this manner, some chemical/dipolar exchange is permitted during a short mixing period in order to allow ^{1}H magnetization to return to water-exposed ^{13}C-/^{15}N-adjacent sites, followed by a selective magnetization transfer to the neighboring ^{13}C or ^{15}N using Lee-Goldburg cross-polarization (LGCP)[94] for optimal selectivity. When used in conjunction with ^{1}H homonuclear decoupling, LGCP slows or prevents dipolar ^{1}H spin

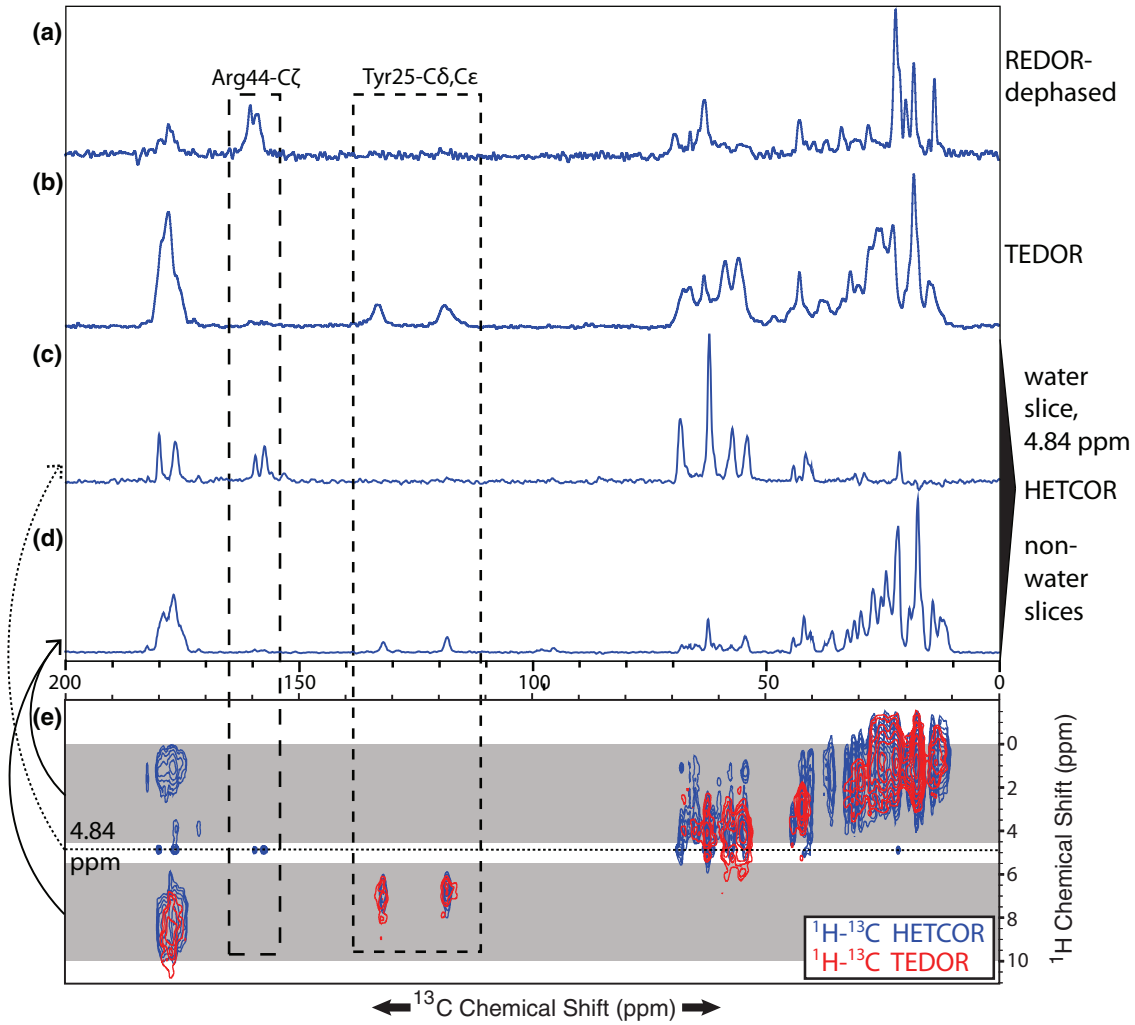

FIG. 4. (a) 1D ^{13}C-REDOR dephasing HETCOR ($4\tau_r$ REDOR blocks with $\tau_r = 55.55\ \mu$s) and (b) ^{1}H–^{13}C TEDOR spectra of Pf1 at 90% RH at 400 MHz and 18 kHz MAS. These spectra are compared with water and non-water slices from a ^{1}H–^{13}C HETCOR ((c) and (d), respectively). The pulse sequences are shown in Figures 1(f), 1(d), and 1(a), respectively. HETCOR and REDOR spectra were acquired without a ^{1}H spin diffusion period and with 900 μs CP contact times. The water (4.84 ppm) slice of a 2D HETCOR spectrum (c) looks very similar to the dephasing HETCOR spectrum (a), while a projection representing the sum of all slices from 0.0 to 4.5 ppm and 5.5 to 7.0 ppm ("non-water") from the same HETCOR spectrum (d) closely resembles the TEDOR spectrum (b), indicating that the pulse sequences work as designed to isolate (REDOR) or remove (TEDOR) magnetization that originates from water. The 159.9 ppm Arg44-Cζ peak is clearly visible in the dephased HETCOR spectrum but absent from the TEDOR spectrum, suggesting a water contact; conversely, the Tyr25–Cδ,Cε peaks are present only in the TEDOR spectra, indicating that the signal originates on a directly bonded ^{1}H–^{13}C pair and not water. Finally, (e) shows an overlay of 2-dimensional ^{1}H–^{13}C TEDOR (red) and HETCOR (blue) spectra; HETCOR peaks that are not reproduced in the TEDOR spectrum are attributable to water contacts and/or chemical exchange. All spectra were taken at 0 °C.

diffusion during cross polarization, further helping to eliminate long-range contacts (Figures 1(b) and 1(i)). Addition of a further DARR homonuclear recoupling element to this pulse sequence permits ^{1}H–^{13}C–^{13}C 3-dimensional spectroscopy, which enables direct assignment of water-exposed residues using a single spectrum. The results, as seen in Figure 6, are similar but not identical to those of the water-selective HETCOR experiment described above. All exchangeable residues observed in water-selective experiments are also seen in MELODI-HETCOR spectra. In addition, a number of non-exchangeable residues (including alanine, valine, isoleucine, and leucine) at the N- and C-termini are observed to be hydrated. Importantly, the cross-peak from hydration water to Arg44-Cζ observed in water-selective HETCOR is faint in ^{1}H–^{13}C MELODI-HETCOR spectra. However, ^{1}H–^{15}N HETCOR spectra (Figure S6 in the supplementary material[100]) clearly show a hydration water cross-peak to both the Arg44 and Lys45 sidechains, each with distinctive ^{15}N chemical shifts. The presence of Lys45 signals is especially notable, as Lys45 is located at the C-terminus of the coat protein and points inward toward the DNA nucleobases in current structural models. As a result, it is expected to be highly hydrated. Its unusually upfield ^{15}N chemical shift of 27.3 ppm is completely outside the range (29.5–43.7 ppm) found in the Biological Magnetic Resonance Data Bank (BMRB),[95] indicative of possible interactions with the DNA (e.g., cation-pi interaction with nucleobases[96]).

Mapping the water-accessible surface

Depiction of the contacts from water-selective and water-filtered experiments on the molecular structure of a Pf1

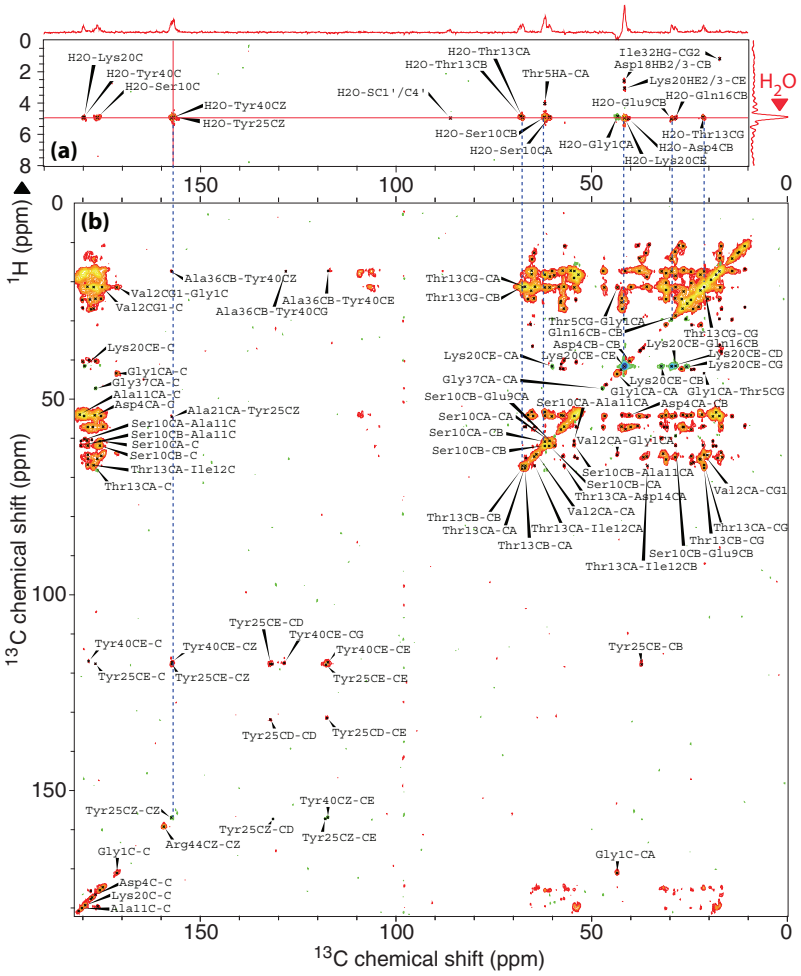

FIG. 5. (a) Water-selective HETCOR and (b) DARR spectra with 100 ms mixing time (pulse sequences shown in Figures 1(g) and 1(h), respectively) of U–^{13}C, ^{15}N Pf1 (90% RH, 5 °C), showing assignments of ^{1}H–^{13}C and ^{13}C–^{13}C cross-peaks by sequential walk and utilizing previously assigned chemical shifts. 1 ms of ^{1}H spin diffusion and 300 μs CP contact times were used. While most water-exposed residues are those with exchangeable protons at the N-terminus, a number of internally facing residues such as Tyr40 and Arg44 also receive magnetization from water.

subunit yields a water-accessibility map as shown in Figure 7, where sites colored in purple are observed in both sets of spectra. In addition to showing the extensive hydration of the coat protein N- and C-termini, maps of the water-accessible surface also reveal the presence of hydrophilic grooves penetrating all the way through the virion's protein coat, large enough to accommodate several water molecules at a time in a chain-like configuration (Figures 7(c) and 7(d)). Similar water chains have recently been proposed for external-internal water exchange in other biomolecular systems, such as myoglobin and BPTI.[10,81] These "tunnels" provide a structural basis for previously reported ion permeability,[51] and help to explain how water is able to access the internal compartments of the virion in order to solvate and stabilize the protein-DNA interface.

Purusottam and co-workers[74] previously investigated the hydration of the Pf1 coat protein in its high temperature form (Pf1^H) using ^{1}H–^{15}N MELODI-HETCOR spectra, finding only seven hydrated residues (S10, A11, K20, A34, S41, R44, and A46). Our data, though acquired on the low-temperature form of Pf1 (Pf1^L), show no evidence of A34 or S41 hydration, despite the fact that S41 has an exchangeable proton and is proximal to Y40 as well as R44. While it is possible that S41 signal could simply be obscured by chemical shift overlap with S10, water-edited ^{13}C–^{13}C DARR spectra would be expected to show characteristic nearest-neighbor cross-peaks for S41 but these peaks are noticeably absent (Figure S9 in the supplementary material[100]). Alanine 34 is located in the middle of a hydrophobic helix in the most hydrophobic region of the coat protein; as a result, it is not expected to be hydrated. It should be noted that Purusottam and co-workers[74] based their assignments only on 2-dimensional ^{1}H–^{15}N correlations and previously published chemical shifts, while the assignments in this work are derived from 3-dimensional ^{1}H–^{13}C–^{13}C data. Carbon, by virtue of its much larger chemical shift dispersion, provides more reliable assignments than nitrogen, and these are further confirmed by intra-residue C–C correlations.

^{1}H spin diffusion reveals magnetization transfer pathways

The preponderance of residues with exchangeable protons in our water accessibility map of Pf1 suggests that chemical exchange is a dominant mechanism of magnetization transfer to/from water under conventional SSNMR

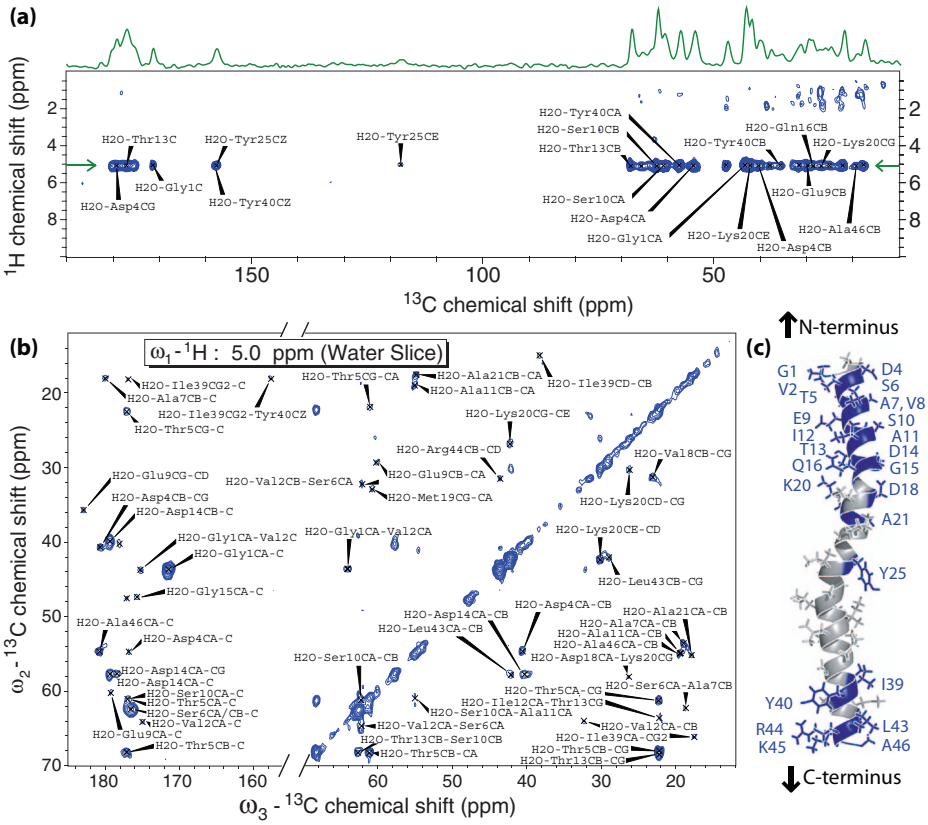

FIG. 6. (a) A ^{1}H–^{13}C MELODI-HETCOR spectrum and (b) the ^{1}H slice of a MELODI-^{1}H–^{13}C–^{13}C 3D (50 ms DARR) spectrum corresponding to water, each acquired at −5 °C and with 8 rotor periods (640 μs) of dephasing on both ^{13}C and ^{15}N, show sets of water contacts similar to that seen in water-selective HETCOR spectra. 1 ms of spin diffusion and 250 μs LGCP contact times were used. (c) A clear spatial pattern of water accessibility can be seen, with virtually all residues at the N-terminus of the coat protein having water contacts, in addition to a cluster of highly hydrated residues (Y40, L43, R44, K45, and A46) at the inward-facing C-terminus. Assigned residues from these spectra, as well as ^{1}H–^{15}N MELODI-HETCOR spectra (Figure S6 in the supplementary material[100]), are labeled in blue on the structure of the Pf1 coat protein. All assignments were performed via backbone walks using multiple 2D and 3D spectra. Assignments of tyrosine spin systems in particular are facilitated by the presence of only 2 aromatic residues in the coat protein, with substantially different backbone chemical shifts. The pulse sequences are shown in Figure 1(i). Available in the supplementary material[100] are the methyl ^{1}H slice of the MELODI-^{1}H–^{13}C–^{13}C 3D spectrum (Figure S7 in the supplementary material[100]) and complementary MELODI-DARR spectra used in assignment (Figure S8 in the supplementary material[100]).

conditions, in agreement with previous studies on other systems.[72,73,80] Because chemical exchange pathways may involve multiple hops between magnetization generation and detection, it is useful to "follow" the progress of magnetization as it undergoes exchange, both to ascertain whether it originated from hydration water and to study its progression. The standard HETCOR pulse sequence places the ^{1}H chemical shift encoding period (t1) immediately preceding the CP element, thereby encoding the endpoint of ^{1}H magnetization ("proximal protons") before being transferred to ^{13}C. When ^{1}H spin diffusion is introduced (SD-HETCOR) however (Figure 1(a)/1(b)), t1 now encodes ^{1}H magnetization before the spin diffusion period, thus encoding where ^{1}H magnetization originated ("remote protons"). In effect, for the case of a simple $^1H_a \rightarrow {}^1H_b \rightarrow {}^{13}C$ magnetization transfer process, SD-HETCOR encodes the chemical shift information of ^1H_a and ^{13}C, while conventional HETCOR provides information about ^1H_b and ^{13}C. Taken together, the spectra represent a pseudo-3D experiment, reporting on both the start and endpoints of ^{1}H magnetization in addition to their ^{13}C correlation. An overlay of HETCOR and SD-HETCOR spectra (Figure S10 in the supplementary material[100]) illustrates the general strategy of tracking ^{1}H magnetization diffusion. For example, G1–C′ and R44-Cζ signal can be seen to originate at the hydration water resonance (SD-HETCOR, "remote protons"), then transfer to protons within 1–2 bonds of the assigned carbon during a 1 ms SD period (HETCOR, "proximal protons" – G1-Hα at 4 ppm and R44-Hζ at 9.5 ppm, respectively), prior to CP transfer to ^{13}C. Numerous studies have shown that water-protein proton exchange occurs on a sub- to low-millisecond timescale, which would allow no more than 1–2 proton hops during 1 ms.[6,80,86] As a result, we can safely assume that our results show a single chemical exchange event, as opposed to some sort of relayed transfer pathway. In contrast, sites that have previously been thought not to interact with water directly (e.g., Y25-CΥ) show no cross-peaks to water in HETCOR or SD-HETCOR spectra, suggesting that they do not receive sufficient magnetization from water or nearby exchangeable protons during 1 ms of spin diffusion.

Additional DNA contacts via HETCOR with long ^{1}H spin diffusion

Having presented a number of band-selective and filtered experiments, which ultimately led to a set of water contacts that makes sense in the context of structural models, we must

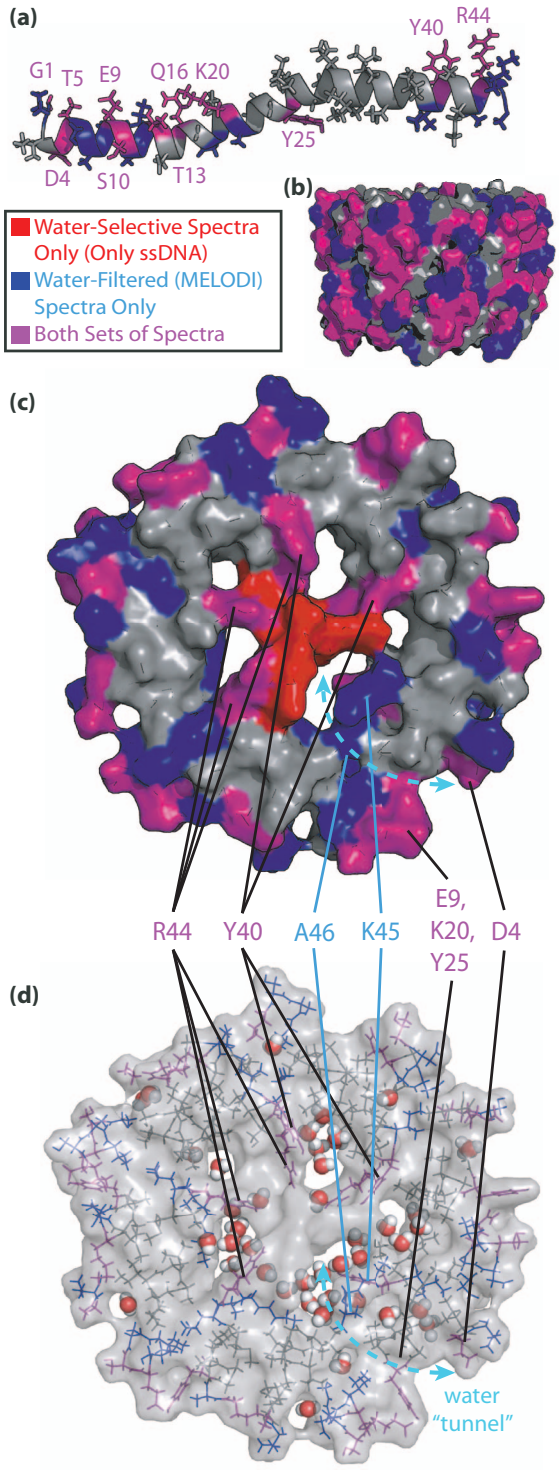

FIG. 7. Water accessibility maps of (a) the Pf1 major coat protein and virion: (b) 20 Å section, viewed from the side; (c) and (d) 5 Å section viewed down the central axis. Coordinates for this consensus model of $Pf1^{L}$ were taken from Tsuboi *et al.*[33] and Straus *et al.*[31] Residues are colored based on the spectrum in which their resonances were observed. Water-exposed residues cluster at the externally exposed N-terminus of the coat protein, forming the hydrophilic grooves seen in (b), as well as at the internal C-terminus facing the DNA (c); the bulk of residues in the middle of the coat protein are not water-accessible. Also noteworthy is the amount of "free" space available to water in the internal cavity of the virion. When solvated in GROMACS[97,98] and subjected to a short MD simulation, several water clusters are apparent (d), in addition to a water chain connecting the exterior of the virion and the internal cavity. The "tunnels" hosting these chains are made up primarily of the water-exposed residues D4, E9, K20, Y25, R44, K45, and A46.

now ask why only the most intense of the Pf1 DNA signals (the sugar C1′/C4′ resonance) was present in water-selective HETCOR spectra. After all, if there are contacts between water and the C-terminal residues of the coat protein that point into the internal cavity, the DNA that sits in this cavity must also be highly hydrated and should also appear. Much of the reason for the faintness of the DNA signals has to do with the fact that the DNA makes up only 6% of the virion's mass, and that the nucleobase signals are further split into their respective types (A/C/G/T). As a result, in order to observe these fainter signals, they must be "enhanced" in some way. One such approach is to put these spins in contact with a much larger magnetization bath, namely, that of hydration water. Practically, this is accomplished by using HETCOR with ^{1}H spin diffusion (SD-HETCOR).[14,99] The SD block spreads ^{1}H polarization, both via NOE mechanisms and by allowing for chemical exchange processes. Because of the likelihood of chemical exchange during this time, it can also be termed a ^{1}H mixing period. SD-HETCOR spectra of Pf1 (Figure S11 in the supplementary material[100]) show a number of additional cross-peaks to the water resonance, including tyrosine Cε and Cδ cross-peaks at 118 and 132 ppm, respectively, along with considerably stronger peaks at 86.5 ppm and 79.8 ppm that can only be assigned as C1′/C4′ and C3′ of the DNA deoxyribose, respectively. The downside of this approach is that the spreading of polarization by definition entails losing selectivity and bringing in peaks that are not directly hydrated via relayed transfers. It is however noteworthy that, with a longer 10 ms SD period, the vast majority of the remaining ^{1}H magnetization originates from the hydration water resonance, with signal from the protons of the coat protein having dramatically diminished in intensity. In this respect, the comparatively slow relaxation properties of water are helpful in isolating water magnetization and thus restoring a measure of selectivity.

The internal hydration water of Pf1

Having shown that hydration water is able to access and transfer magnetization to numerous internally facing residues of the Pf1 coat protein as well as the central DNA, we conclude that this magnetization must either originate on, or at least transfer through, internal hydration water. Based on existing structural models, the distances (10–15 Å) from external hydration water to internally facing waters are too great for efficient magnetization transfer via dipolar mechanisms on timescales of $\leq$1 ms.[99] Because no distinct chemical shift is observed for internal hydration water in any of the aforementioned HETCOR (including SD-HETCOR) spectra, and because selective excitation at the hydration water resonance in water-selective spectroscopy leads to cross-peaks to both internal and external sites, we conclude that the chemical shift of the internal hydration water is degenerate with that of external hydration water, and that the two have similar relaxation properties. However, we must also address the possibility that the two populations could be in fast chemical exchange, possibly via the water "tunnels" depicted in Figures 7(c) and 7(d).

A promising approach to address this latter possibility and isolate strictly signal from internal hydration water has come in the form of PRE – by doping the sample with low concentrations of the well-known paramagnetic relaxant thulium 1,4,7,10-tetraazacyclododecane-1,4,7,10-tetrakis(methylene phosphonate) (TmDOTP), any magnetization from external water is quickly relaxed away. TmDOTP is however far too large (approximately 11 Å across) to penetrate into the internal cavity of the virion and would therefore be unable to directly relax away magnetization arising from the internal hydration water. Enhanced relaxation of internal water contacts, if observed, would only be explainable by quantifiable chemical exchange with external water on the NMR timescale.

Indeed, ^{1}H–^{13}C HETCOR spectra of U–^{13}C, ^{15}N–Pf1 doped with 20 mM TmDOTP prior to precipitation (Figures 8(a)–8(c)) show a marked decrease in overall signal and broadening of most peaks, but retain a notable cross-peak to R44-Cζ at the hydration water resonance (assignment detailed in Figure S12 in the supplementary material[100]). The sidechain of R44, which points into the internal cavity of Pf1, has been previously reported to interact with water.[74] The fact that the peak remains visible and resolved despite all other signals in the spectrum being severely broadened serves as clear evidence of a pool of internal hydration water not directly exposed to TmDOTP. It also demonstrates that chemical exchange between external and internal water is not fast enough to relax away magnetization from internal water until a relatively long SD/mixing period (5 ms) is added to the experiment (Figures 8(d) and 8(e)). A decay curve can be constructed by monitoring the intensity of the R44-Cζ cross-peak as a function of spin diffusion time; when fitted to a single exponential, the data show a decay constant τ of 8.9 $\pm$ 0.4 ms (R = 112.5 $\pm$ 5.1 s^{-1}), suggesting that the exchange process between the hydration water populations occurs on this timescale. When measured in the absence of the

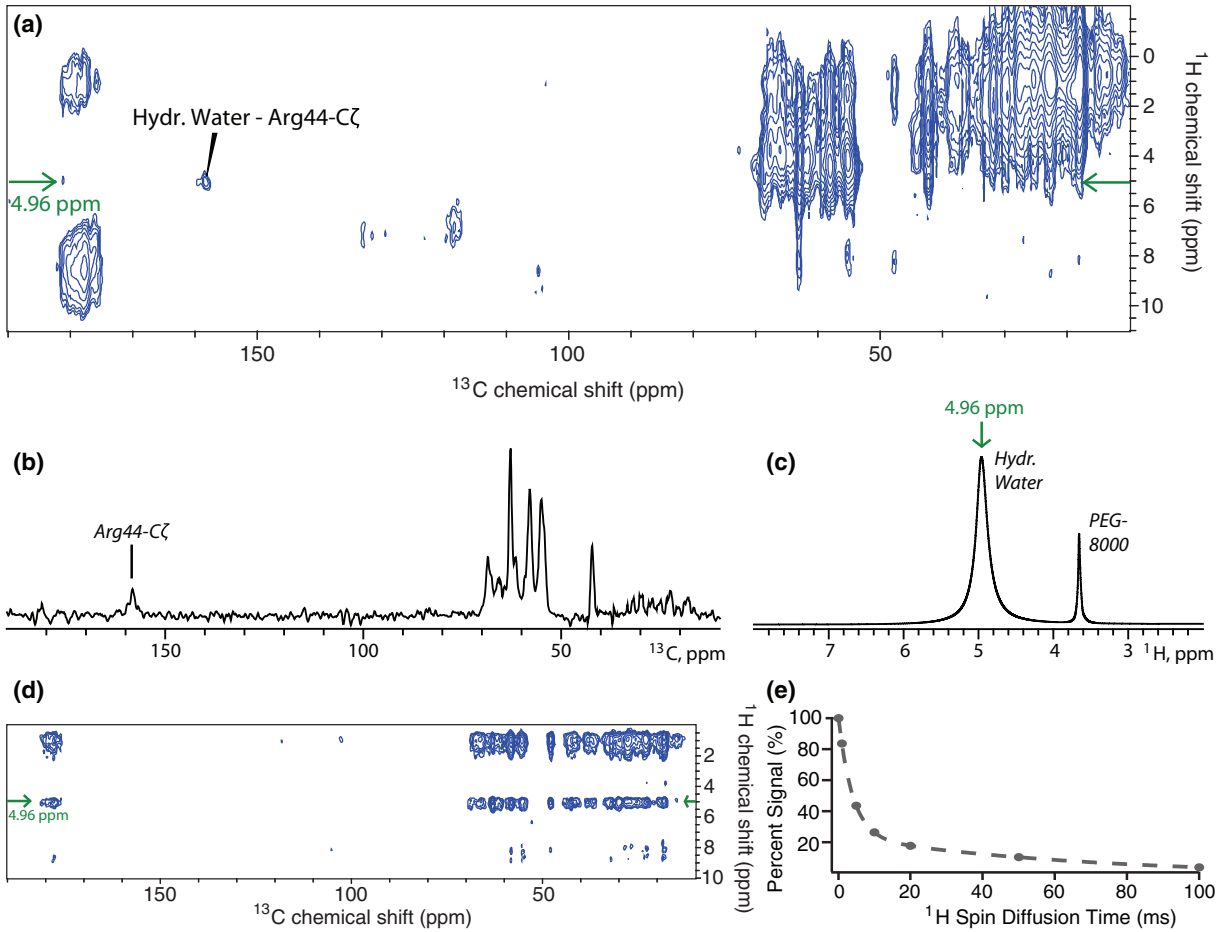

FIG. 8. (a) ^{1}H–^{13}C HETCOR spectrum of U–^{13}C, ^{15}N–Pf1 precipitated in 20 mM TmDOTP and (b) ^{1}H slice from this HETCOR corresponding to hydration water (4.96 ppm). Paramagnetic relaxation enhancement due to the presence of TmDOTP eliminates virtually all direct water-protein cross-peaks, but retains a cross-peak to internally facing Arg44-Cζ, suggesting an internal hydration water population that is not accessible to TmDOTP and that therefore retains magnetization. The linewidths of this peak (^{1}H: 336 Hz, ^{13}C: 385 Hz) are considerably broadened relative to earlier observations of hydration water, presumably due to the influence of TmDOTP, but consistent with the corresponding ^{1}H spectrum of Pf1 in 20 mM TmDOTP shown in (c). It is noteworthy that only hydration water and PEG-8000 peaks are observed in the ^{1}H spectrum; signal from supernatant water and other peaks is suppressed by paramagnetic relaxation enhancement. A SD-HETCOR spectrum of the same sample is shown in (d) with 5 ms of ^{1}H spin diffusion/mixing and ^{1}H homonuclear decoupling (pulse program in Figure 1(b)). As expected, a considerable amount of magnetization now originates at the water resonance, but the previously sharp Arg44-Cζ cross-peak is suppressed, indicative of chemical exchange with water exposed to TmDOTP on this timescale. A decay curve of the Arg44-Cζ signal as a function of SD/mixing time is shown in (e); the decay is well fit using a single exponential (dashed line) with a decay constant of 8.9 ms. Spectra were acquired at $-10\,^{\circ}$C, with 1 ms of ^{1}H spin diffusion and 350 μs CP contact times.

paramagnetic relaxant, the cross-peak intensity increases with SD/mixing times in the range of 0–10 ms, confirming that the decay is due to the presence of TmDOTP. This timescale is similar to but slightly slower than the observed buildup time of water magnetization in SD-HETCOR spectra (e.g., Figure S11 in the supplementary material[100]), which likely indicates that chemical exchange from external hydration water is important to both processes. Observed ^{1}H linewidths of 336 Hz for the R44-Cζ HETCOR cross-peak and 241 Hz for the hydration water resonance in ^{1}H spectra (Figures 8(b) and 8(c)), considerably broader than the normal 100–120 Hz hydration water linewidth, are presumably caused by exchange-mediated paramagnetic relaxation enhancement. Importantly, the finding that chemical exchange between external and internal water occurs on a multi-millisecond timescale indicates that cross-peaks from water to internal protein and DNA sites in HETCOR spectra (with short or no SD) arise primarily directly from internal hydration water, and not via relayed transfers from external water.

CONCLUSIONS

In a series of ^{1}H–^{13}C HETCOR spectra, we have observed a number of water-protein cross-peaks to residues at the C-terminus of the Pf1 coat protein, and, for the first time, detected water-DNA cross-peaks to the same water ^{1}H resonance. These hydration sites are not directly accessible from the outside according to current structural models of the virion. These findings indicate that the interior of the Pf1 capsid is both accessible to water and holds a significant amount of it, in agreement with previous computational and ion accessibility studies.[44,51,52] While we have demonstrated the existence of a population of internal hydration water in Pf1, we also found that its properties are not significantly different from those of external hydration water. Nevertheless, the internal hydration water can be studied by removing magnetization from external hydration water using paramagnetic relaxation enhancement – a promising path forward to unambiguously measure the relaxation properties of this population and gain more insight about its structural role. We also confirm the observation of a water pool in close proximity to the sidechains of the critical C-terminal coat protein residues R44 and K45 (along with several others), which further suggests that internal hydration water is likely a key mediator of the intriguing protein-DNA interactions that stabilize and hold together the remarkably large and highly charged structure.

In addition, we have shown that water-selective and water-filtered SSNMR experiments lead to well-resolved, assignable spectra that can be used to map the water-accessible surfaces of biomolecules. Similar techniques for generating NMR-based water contact maps may be of utility in detecting potential interfaces in docking and drug discovery studies, representing a fruitful extension of SSNMR. These findings will enable and enhance further studies of the protein-DNA interfaces present in the internal cavities of Pf1 and other phages by utilizing water as a convenient magnetization reservoir.

ACKNOWLEDGMENTS

This work was supported by a grant from the National Science Foundation (NSF): MCB 0316248. The authors wish to thank Dr. Benjamin Wylie and Dr. Ségolène Laage for many helpful discussions, as well as Dr. Masamichi Tsuboi for graciously providing unpublished coordinates used for the creation of structural models. The authors would also like to thank Dr. Boris Itin and Dr. Michael Goger of the New York Structural Biology Center for their help with NMR instrumentation.

[1] G. Otting, Prog. Nucl. Magn. Reson. Spectrosc. **31**, 259 (1997).
[2] F. Merzel and J. C. Smith, Proc. Natl. Acad. Sci. U.S.A. **99**, 5378 (2002).
[3] C. Alba-Simionesco, B. Coasne, G. Dosseh, G. Dudziak, K. E. Gubbins, R. Radhakrishnan, and M. Sliwinska-Bartkowiak, J. Phys.-Condens. Matter **18**, R15 (2006).
[4] D. K. Lee, B. S. Kwon, and A. Ramamoorthy, Langmuir **24**, 13598 (2008).
[5] J. Wolfe, G. Bryant, and K. L. Koster, Cryoletters **23**, 157 (2002).
[6] M. Gottschalk, N. A. Dencher, and B. Halle, J. Mol. Biol. **311**, 605 (2001).
[7] B. Halle, V. P. Denisov, and K. Venu, Biol. Magn. Reson. **17**, 419 (2002).
[8] R. Bruschweiler and P. E. Wright, Chem. Phys. Lett. **229**, 75 (1994).
[9] A. Perry, M. P. Stypa, B. K. Tenn, and K. K. Kumashiro, Biophys. J. **82**, 1086 (2002).
[10] S. Kaieda and B. Halle, J. Phys. Chem. B **117**, 14676 (2013).
[11] K. Modig, E. Liepinsh, G. Otting, and B. Halle, J. Am. Chem. Soc. **126**, 102 (2004).
[12] E. K. Paulson, C. R. Morcombe, V. Gaponenko, B. Dancheck, R. A. Byrd, and K. W. Zilm, J. Am. Chem. Soc. **125**, 14222 (2003).
[13] J. Xu, P. Zhu, M. D. Morris, and A. Ramamoorthy, J. Phys. Chem. B **115**, 9948 (2011).
[14] A. B. Siemer, K. Y. Huang, and A. E. McDermott, Proc. Natl. Acad. Sci. U.S.A. **107**, 17580 (2010).
[15] A. J. Wand, M. R. Ehrhardt, and P. F. Flynn, Proc. Natl. Acad. Sci. U.S.A. **95**, 15299 (1998).
[16] N. V. Nucci, M. S. Pometun, and A. J. Wand, Nat. Struct. Mol. Biol. **18**, 245 (2011).
[17] D. H. Live, D. G. Davis, W. C. Agosta, and D. Cowburn, J. Am. Chem. Soc. **106**, 1939 (1984).
[18] C. S. Lee, M. T. Ru, M. Haake, J. S. Dordick, J. A. Reimer, and D. S. Clark, Biotechnol. Bioeng. **57**, 686 (1998).
[19] J. Partridge, P. R. Dennison, B. D. Moore, and P. J. Halling, BBA-Protein Struct. Mol. Enzymol. **1386**, 79 (1998).
[20] Y. G. Mao and Y. Ba, Biophys. J. **91**, 1059 (2006).
[21] A. B. Siemer and A. E. McDermott, J. Am. Chem. Soc. **130**, 17394 (2008).
[22] O. Byl, J. C. Liu, Y. Wang, W. L. Yim, J. K. Johnson, and J. T. Yates, J. Am. Chem. Soc. **128**, 12090 (2006).
[23] E. Mamontov, C. J. Burnham, S. H. Chen, A. P. Moravsky, C. K. Loong, N. R. de Souza, and A. I. Kolesnikov, J. Chem. Phys. **124**, 194703 (2006).
[24] S. A. Lusceac, M. Rosenstihl, M. Vogel, C. Gainaru, A. Fillmer, and R. Bohmer, J. Non-Cryst. Solids **357**, 655 (2011).
[25] J. Swenson and J. Teixeira, J. Chem. Phys. **132**, 014508 (2010).
[26] M. Vogel, Phys. Rev. Lett. **101**, 225701 (2008).
[27] V. P. Denisov and B. Halle, Faraday Discuss. **103**, 227 (1996).
[28] K. Takeya and K. Amako, Virology **28**, 163 (1966).
[29] L. A. Day, C. J. Marzec, S. A. Reisberg, and A. Casadevall, Annu. Rev. Biophys. Biophys. Chem. **17**, 509 (1988).
[30] D. A. Marvin, Curr. Opin. Struct. Biol. **8**, 150 (1998).
[31] S. K. Straus, W. R. P. Scott, C. D. Schwieters, and D. A. Marvin, Eur. Biophys. J. **40**, 221 (2011).
[32] D. S. Thiriot, A. A. Nevzorov, L. Zagyanskiy, C. H. Wu, and S. J. Opella, J. Mol. Biol. **341**, 869 (2004).
[33] M. Tsuboi, M. Tsunoda, S. A. Overman, J. M. Benevides, and G. J. Thomas, Biochemistry **49**, 1737 (2010).
[34] L. A. Day, R. L. Wiseman, and C. J. Marzec, Nucl. Acids Res. **7**, 1393 (1979).
[35] C. J. Marzec and L. A. Day, Biophys. J. **67**, 2205 (1994).
[36] D. J. Liu and L. A. Day, Science **265**, 671 (1994).
[37] I. V. Sergeyev, L. A. Day, A. Goldbourt, and A. E. McDermott, J. Am. Chem. Soc. **133**, 20208 (2011).

[38]M. Zweckstetter and A. Bax, J. Biomol. NMR **20**, 365 (2001).
[39]M. R. Hansen, L. Mueller, and A. Pardi, Nat. Struct. Biol. **5**, 1065 (1998).
[40]E. J. Wachtel, F. J. Marvin, and D. A. Marvin, J. Mol. Biol. **107**, 379 (1976).
[41]D. S. Thiriot, A. A. Nevzorov, and S. J. Opella, Protein Sci. **14**, 1064 (2005).
[42]L. Specthrie, J. Greenberg, M. J. Glucksman, J. Diaz, and L. Makowski, Biophys. J. **52**, 199 (1987).
[43]O. M. Astley and A. M. Donald, Biomacromolecules **2**, 672 (2001).
[44]J. L. Lorieau, L. A. Day, and A. E. McDermott, Proc. Natl. Acad. Sci. U.S.A. **105**, 10366 (2008).
[45]J. H. Wang, J. Am. Chem. Soc. **77**, 258 (1955).
[46]H. R. Drew and R. E. Dickerson, J. Mol. Biol. **151**, 535 (1981).
[47]M. Falk, R. C. Lord, and K. A. Hartman, J. Am. Chem. Soc. **84**, 3843 (1962).
[48]I. Brovchenko, A. Krukau, A. Oleinikova, and A. K. Mazur, J. Phys. Chem. B **111**, 3258 (2007).
[49]A. J. Rowe, Biophys. Chem. **93**, 93 (2001).
[50]J. H. Wang, J. Am. Chem. Soc. **76**, 4755 (1954).
[51]A. Casadevall and L. A. Day, Biochemistry **22**, 4831 (1983).
[52]A. Casadevall and L. A. Day, Nucl. Acids Res. **10**, 2467 (1982).
[53]S. Moon and D. A. Case, J. Biomol. NMR **38**, 139 (2007).
[54]A. McDermott, Annu. Rev. Biophys. **38**, 385 (2009).
[55]M. Renault, A. Cukkemane, and M. Baldus, Angew. Chem., Int. Ed. Engl. **49**, 8346 (2010).
[56]G. M. Clore, A. Bax, P. T. Wingfield, and A. M. Gronenborn, Biochemistry **29**, 5671 (1990).
[57]G. Otting and K. Wuthrich, J. Am. Chem. Soc. **111**, 1871 (1989).
[58]L. Calucci, C. Forte, L. Galleschi, M. Geppi, and S. Ghiringhelli, Int. J. Biol. Macromol. **32**, 179 (2003).
[59]G. S. Harbison, J. E. Roberts, J. Herzfeld, and R. G. Griffin, J. Am. Chem. Soc. **110**, 7221 (1988).
[60]A. S. Kulik, J. R. C. Decosta, and J. Haverkamp, J. Agr. Food Chem. **42**, 2803 (1994).
[61]D. Radloff, C. Boeffel, and H. W. Spiess, Macromolecules **29**, 1528 (1996).
[62]F. Separovic, Y. H. Lam, X. Ke, and H. K. Chan, Pharm. Res. **15**, 1816 (1998).
[63]V. Chevelkov, K. Faelber, A. Diehl, U. Heinemann, H. Oschkinat, and B. Reif, J. Biomol. NMR **31**, 295 (2005).
[64]B. Grunberg, T. Emmler, E. Gedat, I. Shenderovich, G. H. Findenegg, H. H. Limbach, and G. Buntkowsky, Chemistry **10**, 5689 (2004).
[65]H. Van Melckebeke, P. Schanda, J. Gath, C. Wasmer, R. Verel, A. Lange, B. H. Meier, and A. Bockmann, J. Mol. Biol. **405**, 765 (2011).
[66]E. E. Wilson, A. Awonusi, M. D. Morris, D. H. Kohn, M. M. Tecklenburg, and L. W. Beck, Biophys. J. **90**, 3722 (2006).
[67]A. Bockmann, C. Gardiennet, R. Verel, A. Hunkeler, A. Loquet, G. Pintacuda, L. Emsley, B. H. Meier, and A. Lesage, J. Biomol. NMR **45**, 319 (2009).
[68]A. Bockmann, M. Juy, E. Bettler, L. Emsley, A. Galinier, F. Penin, and A. Lesage, J. Biomol. NMR **32**, 195 (2005).
[69]M. Ernst, A. P. M. Kentgens, and B. H. Meier, J. Magn. Reson. **138**, 66 (1999).
[70]J. Jeener, B. H. Meier, P. Bachmann, and R. R. Ernst, J. Chem. Phys. **71**, 4546 (1979).
[71]A. Lesage and A. Bockmann, J. Am. Chem. Soc. **125**, 13336 (2003).
[72]A. Lesage, L. Emsley, F. Penin, and A. Bockmann, J. Am. Chem. Soc. **128**, 8246 (2006).
[73]A. Lesage, C. Gardiennet, A. Loquet, R. Verel, G. Pintacuda, L. Emsley, B. H. Meier, and A. Bockmann, Angew. Chem., Int. Ed. Engl. **47**, 5851 (2008).
[74]R. N. Purusottam, R. K. Rai, and N. Sinha, J. Phys. Chem. B **117**, 2837 (2013).
[75]A. Goldbourt, B. J. Gross, L. A. Day, and A. E. McDermott, J. Am. Chem. Soc. **129**, 2338 (2007).
[76]B. M. Fung, A. K. Khitrin, and K. Ermolaev, J. Magn. Reson. **142**, 97 (2000).
[77]B. Elena, G. de Paëpe, and L. Emsley, Chem. Phys. Lett. **398**, 532 (2004).
[78]X. L. Yao, K. Schmidt-Rohr, and M. Hong, J. Magn. Reson. **149**, 139 (2001).
[79]J. Newman, L. A. Day, G. W. Dalack, and D. Eden, Biochemistry **21**, 3352 (1982).
[80]E. Liepinsh and G. Otting, Magn. Reson. Med. **35**, 30 (1996).
[81]F. Persson and B. Halle, J. Am. Chem. Soc. **135**, 8735 (2013).
[82]H. J. Steinhoff, B. Kramm, G. Hess, C. Owerdieck, and A. Redhardt, Biophys. J. **65**, 1486 (1993).
[83]M. P. Williamson, Annu. Rep. NMR Spectrosc. **65**, 77 (2009).
[84]B. Halle, Philos. Trans. R. Soc. B **359**, 1207 (2004).
[85]J. M. Lopez del Amo, U. Fink, and B. Reif, J. Biomol. NMR **48**, 203 (2010).
[86]K. Venu, V. P. Denisov, and B. Halle, J. Am. Chem. Soc. **119**, 3122 (1997).
[87]S. W. Englander, N. W. Downer, and H. Teitelbaum, Annu. Rev. Biochem. **41**, 903 (1972).
[88]Y. W. Bai, J. S. Milne, L. Mayne, and S. W. Englander, Proteins **17**, 75 (1993).
[89]S. W. Englander, T. R. Sosnick, J. J. Englander, and L. Mayne, Curr. Opin. Struct. Biol. **6**, 18 (1996).
[90]C. P. Butts, C. R. Jones, E. C. Towers, J. L. Flynn, L. Appleby, and N. J. Barron, Org. Biomol. Chem. **9**, 177 (2011).
[91]M. Etzkorn, S. Martell, O. C. Andronesi, K. Seidel, M. Engelhard, and M. Baldus, Angew. Chem., Int. Ed. **46**, 459 (2007).
[92]S. Y. Liao, K. J. Fritzsching, and M. Hong, Prot. Sci. **22**, 1623 (2013).
[93]S. H. Li, Y. C. Su, W. B. Luo, and M. Hong, J. Phys. Chem. B **114**, 4063 (2010).
[94]V. Ladizhansky and S. Vega, J. Chem. Phys. **112**, 7158 (2000).
[95]E. L. Ulrich, H. Akutsu, J. F. Doreleijers, Y. Harano, Y. E. Ioannidis, J. Lin, M. Livny, S. Mading, D. Maziuk, Z. Miller, E. Nakatani, C. F. Schulte, D. E. Tolmie, R. Kent Wenger, H. Yao, and J. L. Markley, Nucl. Acids Res. **36**, D402 (2008).
[96]E. V. Pletneva, A. T. Laederach, D. B. Fulton, and N. M. Kostic, J. Am. Chem. Soc. **123**, 6232 (2001).
[97]H. J. C. Berendsen, D. Vanderspoel, and R. Vandrunen, Comput. Phys. Commun. **91**, 43 (1995).
[98]S. Pronk, S. Pall, R. Schulz, P. Larsson, P. Bjelkmar, R. Apostolov, M. R. Shirts, J. C. Smith, P. M. Kasson, D. van der Spoel, B. Hess, and E. Lindahl, Bioinformatics **29**, 845 (2013).
[99]K. K. Kumashiro, K. Schmidt-Rohr, O. J. Murphy, K. L. Ouellette, W. A. Cramer, and L. K. Thompson, J. Am. Chem. Soc. **120**, 5043 (1998).
[100]See supplementary material at http://dx.doi.org/10.1063/1.4903230 for approximate water/protein ratios in Pf1 at different hydration levels; hexagonal close packing model of dense Pf1 precipitates; ^{13}C-REDOR dephasing curves of ^{1}H populations; confirmation of assignment for water populations (supernatant removal, temperature series, 2D exchange spectroscopy); overlay of Pf1 ^{13}C–^{13}C DARR and water-selective DARR spectra, illustrating the absence of S41 cross-peaks in the latter; ^{1}H–^{15}N MELODI-HETCOR spectrum of Pf1 showing key water-accessible ^{15}N sites; methyl ^{1}H slice of MELODI–^{1}H–^{13}C–^{13}C 3D spectrum; ^{13}C–^{13}C MELODI-DARR (25 and 100 ms mixing times) spectra of U–^{13}C, ^{15}N–Pf1; Pf1 HETCOR spectra with ^{1}H spin diffusion, including buildup curves; 2D DARR spectrum (50 ms mixing) of U–^{13}C, ^{15}N Pf1 in the presence of paramagnetic relaxant TmDOTP; full acquisition and processing parameters for all spectra presented (1D, 2D, 3D).